

Enhanced Myocardial Glucose Use in Patients with a Deficiency in Long-Chain Fatty Acid Transport (CD36 Deficiency)

Kazuki Fukuchi, Shuichi Nozaki, Tohru Yoshizumi, Shinji Hasegawa, Toshiisa Uehara, Tsutomu Nakagawa, Tohru Kobayashi, Yoshiaki Tomiyama, Shizuya Yamashita, Yuji Matsuzawa and Tsunehiko Nishimura

Division of Tracer Kinetics, Biomedical Research Center; Second Department of Internal Medicine; Osaka University Medical School, Suita; Department of Radiology, Minoh City Hospital, Minoh; Department of Cardiology, Osaka Medical Center for Cancer and Cardiovascular Diseases, Osaka, Japan

CD36 is a multifunctional, 88 kDa glycoprotein that is expressed on platelets and monocytes/macrophages. CD36 also has high homology with the long-chain fatty acid (LFA) transporter in the myocardium. Although platelet and monocyte CD36 levels can indicate a CD36 deficiency, they cannot predict specific clinical manifestations in the myocardium of a given person. We examined the hypothesis that a deficiency in LFA transport augments myocardial glucose uptake in patients with a type I CD36 deficiency. **Methods:** Seven fasting patients with a type I CD36 deficiency and 9 controls were assessed by cardiac radionuclide imaging using beta-methyl-p-iodophenyl-pentadecanoic acid (BMIPP) as a LFA tracer and by PET with ^{18}F -fluorodeoxyglucose (FDG). **Results:** None of the patients with a CD36 deficiency showed myocardial uptake of BMIPP. The percentage dose uptake of BMIPP in these subjects was significantly lower than that in normal controls (1.31 ± 0.24 versus 2.90 ± 0.2 ; $P < 0.005$). PET studies revealed that myocardial FDG accumulation was substantially increased in patients with a CD36 deficiency. Quantitative analysis showed that the percentage dose uptake of FDG in patients with a CD36 deficiency was significantly higher than that in normal controls (1.28 ± 0.35 versus 0.43 ± 0.22 ; $P < 0.01$). **Conclusion:** CD36 functions as a major myocardial LFA transporter and its absence may cause a compensatory upregulation of myocardial glucose uptake.

Key Words: CD36 deficiency; beta-methyl-p-iodophenyl-pentadecanoic acid; fluorodeoxyglucose

J Nucl Med 1999; 40:239–243

CD36 is a glycoprotein with a molecular weight of 88 kDa that is expressed on platelets, monocytes/macrophages, capillary endothelial cells and adipocytes (1). CD36 may be a multifunctional molecule that harbors receptors for collagen (2), thrombospondin (3), malaria-infected erythrocytes (4) and oxidized low-density lipoprotein. Some patients are deficient in platelet CD36 (5). Because these patients have no obvious hemostatic problems, CD36 does not seem to be

essential for platelet function. CD36 also has high homology with the long-chain fatty acid (LFA) transporter in the myocardium (6,7). Although platelet and monocyte CD36 levels can indicate a CD36 deficiency, specific clinical manifestations in a given patient remain undefined.

This study investigates the role of CD36 as a metabolic substrate transporter in the myocardium and examines the hypothesis that a CD36 deficiency augments myocardial glucose uptake. We applied cardiac radionuclide imaging by using beta-methyl-p-iodophenyl-pentadecanoic acid (BMIPP) as a tracer of LFA and PET scanning with ^{18}F -fluorodeoxyglucose (FDG) on the assumption that the latter variable yields direct evidence of the glucose metabolic state in patients with a CD36 deficiency.

MATERIALS AND METHODS

Seven unrelated persons (mean age 63.5 ± 4.2 y) participated in this study (Table 1). BMIPP scintigraphy initially revealed negative myocardial accumulation in 3 of them, so we analyzed CD36 expression on their platelets and monocytes. The remaining 4 participants were identified by blood screening for CD36 expression. We confirmed that all participants had a type I CD36 deficiency (neither platelets nor monocytes express CD36). Five of the 7 participants underwent coronary angiography because of their cardiac symptoms, and coronary artery disease (CAD) was diagnosed in 4 of the participants. Of the remaining 3 participants, 1 was evaluated by echocardiography as having hypertrophic cardiomyopathy and 2 participants were hypertensive.

A normal BMIPP and FDG uptake database was constructed on the basis of information gathered from 9 age-matched healthy volunteers (average age 58.0 ± 4.2 y) with no signs, symptoms or electrocardiographic evidence of heart disease. None had taken medication for at least 2 wk before the study.

Written informed consent was obtained from each participant. The study protocol was approved by the standard ethical guidelines of the Osaka University Medical School and the collaborating institutions.

Flow Cytometric Analysis

CD36 expression on platelets and monocytes was analyzed by flow cytometry and the type of deficiency was determined as described (8). In brief, a $50 \mu\text{L}$ suspension of platelets ($2 \times 10^5 \mu\text{L}$) or mononuclear cells ($2 \times 10^4 \mu\text{L}$) was incubated for 30 min with 5

Received Mar. 4, 1998; revision accepted May 28, 1998.

For correspondence or reprints contact: Tsunehiko Nishimura, MD, PhD, Division of Tracer Kinetics, Biomedical Research Center, Osaka University, Medical School, Yamada-oka 2-2 Suita, Osaka, 565-0871 Japan.

TABLE 1
Summary of Patients with Type I CD36 Deficiency

Patient no.	Sex	Age (y)	Diagnosis	Coronary angiogram	Wall motion	(Exercise or rest) ²⁰¹ Tl imaging
1	F	63	CAD	(7) 99%; (12) 90%	Normal	(Exercise) Redistribution in anteroseptal wall
2	M	72	CAD—post PTCA	(11) 75%–20%; (12) 90%–20%	NA	(Rest) Inferoposterior wall defect at rest
3	F	51	Hypertension	NA	Normal	(Exercise) Normal perfusion
4	M	57	Hypertrophic cardiomyopathy	Normal	Normal	(Exercise) Normal perfusion
5	M	60	CAD—post PTCA	(1) 99%; (2) 90% to 75%	Lateral wall hypokinesis	(Exercise) Slight reverse redistribution in posterolateral wall
6	M	63	Hypertension	NA	Normal	(Exercise) Normal perfusion
7	M	71	CAD	(5) 90%; (11) 75%; (12) 90%	Anterior and lateral wall akinesis	(Rest) Anteroseptal and inferoposterior wall defect at rest

Segmental numbers are in parentheses.

CAD = coronary artery disease; PTCA = percutaneous transluminal coronary angioplasty; NA = not available.

μL of fluorescein isothiocyanate (FITC)-labeled antihuman CD36 monoclonal antibody (OKM5; Ortho Diagnostic System Inc., Raritan, NJ) or FITC-labeled control IgG. Cells were then diluted to 400 μL in Tris-buffered saline and analyzed with a FACScan (Becton Dickinson and Co., Sunnyvale, CA).

BMIPP Study

The myocardial uptake of BMIPP was calculated by applying a modification of the Ishii-MacIntyre method (9,10). Patients fasted overnight, then an 18-gauge nonstick-coated catheter was placed in the anterior-cubital vein. The patients were placed in a supine position facing a gamma camera equipped with a parallel-hole, high-resolution collimator (RC-2000; Hitachi Medical Co. Ltd., Tokyo, Japan). A dose of 111 MBq (3 mCi) BMIPP was intravenously injected and rapidly flushed with 20 mL saline. Serial dynamic imaging from the standard anterior projection was started at a rate of 1 frame/s over the whole thorax and continued for 60 s. The total injected dose was obtained from the peak counts of the time-activity curve over the whole thorax. On the anterior planar image obtained over 5 min with another gamma camera (GCA9300HG/A; Toshiba Co. Ltd., Tokyo, Japan), regions of interest (ROIs) were manually drawn over the entire left ventricle and mediastinum (background) with reference to images from a ²⁰¹Tl perfusion scan. Total counts and the number of pixels within the myocardial ROI and background ROI were determined. Myocardial BMIPP uptake was calculated as follows:

BMIPP uptake index (%)

$$= (M1 - M2 \times A1/A2)/T \times 300 \times Cf, \quad \text{Eq. 1}$$

where M1 = counts in myocardial ROI (counts); M2 = counts in background (counts); A1 = number of pixels in myocardial ROI (pixels); A2 = number of pixels in background (pixels); T = total injected dose per second (pixel/s); and Cf = calibration factor between two gamma camera systems.

An additional myocardial SPECT scan was performed after anterior planar image acquisition. SPECT images were obtained 30 min after BMIPP administration and data were acquired as follows. A rotating triple-headed gamma camera equipped with a low-

energy, general-purpose collimator, interfaced with a dedicated computer, collected SPECT data from 20 projections over 360° for 60 s per projection for a total of 20 min. Energy was discriminated with a 20% window centered over a 160-keV photopeak. Images were acquired on a 64 × 64 matrix and stored on a hard disk for further processing. Data were preprocessed with a Butterworth filter, and the transaxial images were reconstructed with a Shepp and Logan filter. Attenuation correction was not performed.

Exercise-redistribution or rest ²⁰¹Tl myocardial perfusion images were obtained on a different day.

FDG PET Study

FDG PET was performed on each participant on different days from SPECT imaging after fasting for at least 15 h. After transmission scanning for attenuation correction, 320–370 MBq (8.6–10 mCi) FDG was intravenously injected. Forty-five minutes later, static emission scanning was performed for 10 min. The blood concentrations of glucose, insulin and free fatty acid were evaluated by using samples obtained before tracer injection. PET scanning was performed with a HEADTOME V (Shimadzu Co. Ltd., Kyoto, Japan).

Myocardial FDG uptake was quantified as described (11,12). Briefly, PET data were reconstructed into transaxial cardiac planes. ROIs of ≥600 pixels were manually drawn, including the entire left ventricular wall, and the average ROI count in the center slice of myocardial cross-sectional images was obtained. The percentage dose uptake of FDG was calculated as the ROI count divided by the injection dose, with cross-calibration factor and decay corrections. The formula used to calculate percentage dose uptake was as follows:

FDG uptake index (% dose of 60 kg of BW)

$$= [Ct/(D \times CF \times 60/BW)] \times 100(\%), \quad \text{Eq. 2}$$

where Ct = average myocardial tissue activity (cps/mL); D = injected dose; BW = the person's body weight; CF = the calibration factor between MBq on the curie meter and cps/mL on the PET images.

Statistical Analysis

Data are expressed as mean \pm SD. Results were compared between groups with Student *t* tests; $P < 0.05$ was considered significant.

RESULTS

Flow cytometric results typical of patients with a type I CD36 deficiency and of healthy volunteers are shown in Figure 1. The anti-CD36 antibody OKM5 bound to platelets and monocytes obtained from controls (upper panel), but not to those of patients with a type I CD36 deficiency (lower panel).

Representative planar BMIPP, BMIPP SPECT FDG PET and ^{201}Tl SPECT myocardial images obtained from a control person and from a person with a type I CD36 deficiency are shown in Figure 2. Myocardial planar BMIPP images from the controls were normal, whereas those from CD36-deficient patients revealed significantly reduced myocardial BMIPP accompanied by obvious hepatic uptake. The mean myocardial BMIPP uptake of patients with a type I CD36 deficiency was $1.31\% \pm 0.24\%$, which was significantly lower than that of normal controls ($2.90\% \pm 0.2\%$; $P < 0.005$) (Fig. 3).

PET images showed that FDG uptake levels were low in fasting control participants (% uptake 0.43 ± 0.22 ; $P < 0.01$) but were significantly increased in patients with a type I CD36 deficiency (% uptake 1.28 ± 0.35) (Figs. 2 and 3).

Table 2 shows the results of the blood tests performed at the time of FDG PET examination. There are no significant differences in serum glucose, insulin or free fatty acid levels between normal controls and patients with a CD36 deficiency.

DISCUSSION

In this study, we examined the hypothesis that a deficiency in LFA transport augments myocardial glucose

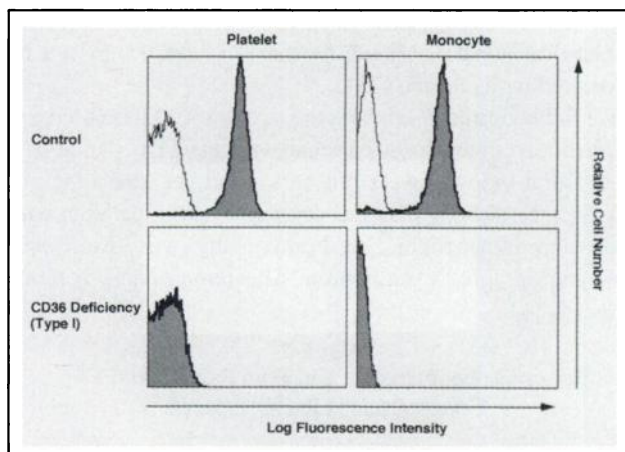


FIGURE 1. Flow cytometric analysis to determine surface expression of CD36 on platelets and monocytes from controls (upper panels) and patients with type I CD36 deficiency (lower panels). Immunofluorescent pattern with antihuman CD36 monoclonal antibody (shaded portion) or with control IgG (unshaded portion).

uptake in patients with a CD36 deficiency. We confirmed that patients with a type I CD36 deficiency have greatly reduced myocardial LFA uptake and discovered that glucose uptake is augmented under fasting conditions.

CD36 as Long-Chain Fatty Acid Transporter

CD36 deficiency was originally identified in a patient who was refractory to platelet transfusion (13,14). Platelet CD36 deficiency has been identified in about 3% and 0.3% of the Japanese (13) and American populations (5), respectively. Because patients are almost always healthy and do not present with obvious hemostatic diseases, the essential function of CD36 has not been defined. A connection between CD36 and membrane fatty acid transporter protein has been established (6,7). Therefore, whether or not the fatty acid transport system functionally changes and consequently disrupts energy metabolism in patients with a CD36 deficiency should be investigated.

The lipophilic character of fatty acids suggests that they diffuse directly through the phospholipid bilayer of the plasma membrane. Thus, it has been considered that fatty acids are absorbed by passive diffusion (15,16). However, the recent identification of a membrane-associated fatty acid transport system in hepatocytes (17,18) has led to the notion that myocardial fatty acid uptake is also mediated by a carrier protein. Abumrad et al. (7) have identified and cloned an 88-kDa adipocyte membrane fatty acid transporter protein that was specifically labeled with LFA derivatives. They also showed that the amino acid sequence of this protein was 85% homologous to that of human CD36 (19).

^{123}I -BMIPP in Patients with CD36 Deficiency

BMIPP is an iodinated analog of pentadecanoic acid that is transported into the myocardium in a manner similar to that of LFA, so it has been proposed as an LFA probe for myocardial fatty acid metabolism. BMIPP is rapidly incorporated into the triglyceride pool and is metabolized by initial beta-oxidation and subsequent cycles of alpha-oxidation (20). The slow washout kinetics of this tracer from the myocardium mainly reflect the turnover rate of the triglyceride pool in the cytosol (21). As mentioned previously, kinetic studies of the isolated perfused (20) or in vivo rat heart (21) have clarified the metabolic pathway of BMIPP, but the mechanism of uptake has not been investigated. In this study, none of the patients with a type I CD36 deficiency showed myocardial BMIPP uptake. This finding indicates that patients with a type I CD36 deficiency lack the LFA transporter and that BMIPP uptake is mediated by the LFA transporter system.

Myocardial Glucose Use in Patients with CD36 Deficiency

Myocardial FDG uptake was significantly higher in patients with a type I CD36 deficiency than in healthy volunteers, suggesting that more glucose is used by the CD36 deficient group. In the fasting state, when plasma glucose levels are reduced and insulin levels are low, the normal myocardium uses relatively little glucose and prefer-

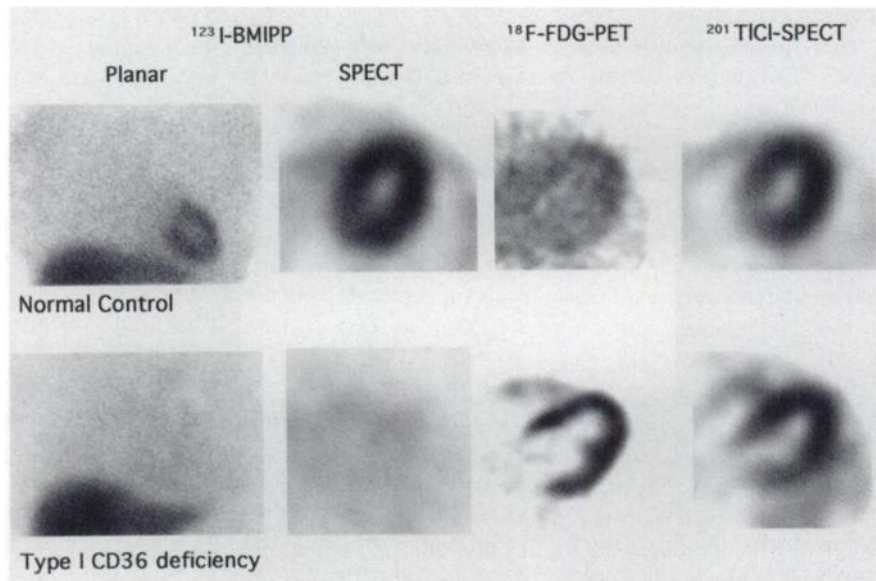


FIGURE 2. Myocardial images with BMIPP, FDG and ^{201}Tl . Upper panel: normal control. Lower panel: patient with type I CD36 deficiency.

entally uses free fatty acids for energy production. This study indicates that the relationship between LFA metabolism and glucose use functions at the level of the transporter system. In addition, glucose uptake is upregulated to compensate for the deficient membrane fatty acid transport. The reason why the myocardium with an LFA transporter deficiency has augmented myocardial glucose uptake remains unknown. If myocardial LFA transport is defective, the myocardium can use other fatty acids such as medium- or short-chain molecules because myocardial LFAs do not function in the uptake of short- and medium-chain fatty acids (17). Tanaka and Kawamura (22) have reported that sulfo-N-succinimidyl derivatives of palmitic acid, which bind to a membrane protein and inhibit the transporter, reduce myocardial ^{14}C -palmitate uptake but increase myocardial ^{14}C -D-glucose uptake in isolated perfused rat hearts.

Limitations

Planar images of patients with a type I CD36 deficiency show negative myocardial BMIPP uptake. However, we found that the percentage myocardial BMIPP uptake was not

zero because of the high BMIPP background. BMIPP dynamics in the normal heart are characterized by high myocardial uptake, a relatively high heart-to-background count ratio and rapid blood clearance (23). However, when myocardial BMIPP uptake is negative, counts in the blood pool are relatively high and interfere with quantitative analyses.

Our study population included 4 patients with chronic CAD. Myocardial BMIPP accumulation is decreased compared with flow tracer in acute and subacute myocardial infarction and in unstable angina (24,25) and the myocardium accumulates enhanced levels of FDG under fasting conditions (26,27). However, all patients with CAD in this study had a normal perfused myocardial segment according to redistribution images of exercise-redistribution or rest ^{201}Tl scintigraphy. Thus, the reduced BMIPP uptake and augmented FDG uptake in the entire myocardium without any stenotic coronary artery segments or evidence of global myocardial ischemia shown by the ^{201}Tl study may not be associated with chronic CAD.

We did not directly confirm the status of CD36 expression in cardiomyocytes from patients with a CD36 deficiency. Myocardial biopsies were not performed because a lack of CD36 expression by platelets or monocytes in patients with CAD and hypertrophic cardiomyopathy was discovered after angiographic examination. The remaining 2 patients

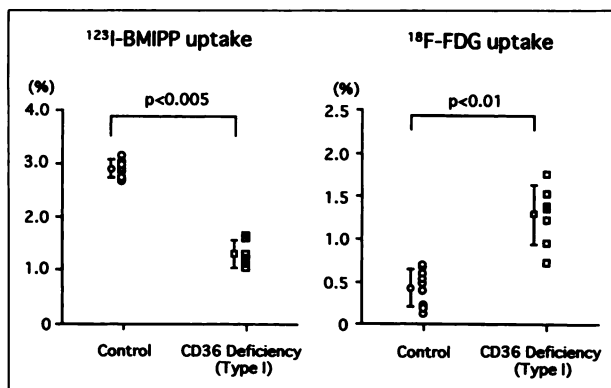


FIGURE 3. Comparison of percentage dose uptake of BMIPP and FDG between controls and patients with type I CD36 deficiency.

TABLE 2
Serum Glucose, Insulin and Free Fatty Acid (FFA) Concentrations in Participants

	Serum glucose (mg/dL)	Insulin ($\mu\text{U/mL}$)	FFA ($\mu\text{Eq/L}$)
Normal control (n = 9)	95.0 \pm 8.1	5.8 \pm 5.6	411.8 \pm 138.3
Subjects with CD36 deficiency (n = 7)	106.0 \pm 26.1	5.2 \pm 4.3	611.3 \pm 243.7
P value	0.25	0.82	0.32

did not require angiography because they did not exhibit any symptoms associated with heart disease other than hypertension. Isolation of the myocardial LFA transporter from bovine hearts has revealed that LFA is highly homologous to human CD36 (6). Thus, it is likely that patients with a CD36 deficiency do not have CD36 on their myocardium.

CONCLUSION

These results indicate that CD36 functions as a major myocardial LFA transporter and that its absence causes the compensatory upregulation of myocardial glucose use.

ACKNOWLEDGMENTS

We thank the staff of the Division of Nuclear Medicine, Osaka University Medical School Hospital and the Department of Radiology, Minoh City Hospital for their technical support with the ¹²³I-BMIPP and ¹⁸F-FDG PET myocardial studies. We also thank Ms. Norma Foster for critical reading of the article.

REFERENCES

- Greenwalt DE, Lipsky RH, Ockenhouse CF, Ikeda H, Tandon NN, Jamieson GA. Membrane glycoprotein CD36: a review of its roles in adherence, signal transduction, and transfusion medicine. *Blood*. 1992;80:1105-1115.
- Tandon NN, Kralisz U, Jamieson GA. Identification of glycoprotein IV (CD36) as a primary receptor for platelet-collagen adhesion. *J Biol Chem*. 1989;264:7576-7583.
- Asch AS, Barnwell J, Silverstein RL, Nachman RL. Isolation of the thrombospondin membrane receptor. *J Clin Invest*. 1987;79:1054-1061.
- Oquendo P, Hundt E, Lawler J, Seed B. CD36 directly mediates cytoadherence of *Plasmodium falciparum* parasitized erythrocytes. *Cell*. 1989;58:95-101.
- Yamamoto N, Akamatsu N, Sakuraba H, Yamazaki H, Tanoue K. Platelet glycoprotein IV (CD36) deficiency is associated with the absence (type I) or the presence (type II) of glycoprotein IV on monocytes. *Blood*. 1994;83:392-397.
- Tanaka T, Kawamura K. Isolation of myocardial membrane long-chain fatty acid-binding protein: homology with a rat membrane protein implicated in the binding or transport of long-chain fatty acids. *J Mol Cell Cardiol*. 1995;27:1613-1622.
- Abumrad NA, el-Maghrabi MM, Amri EZ, Lopez E, Grimaldi PA. Cloning of a rat adipocyte membrane protein implicated in binding or transport of long-chain fatty acids that is induced during preadipocyte differentiation. Homology with human CD36. *J Biol Chem*. 1993;268:17665-17668.
- Take H, Kashiwagi H, Tomiyama Y, et al. Expression of GPIV and N(aka) antigen on monocytes in N(aka)-negative individuals whose platelets lack GPIV. *Br J Haematol*. 1993;84:387-391.
- Fujiwara S, Takeishi Y, Atsumi H, Takahashi K, Tomoike H. Fatty acid metabolic imaging with iodine-123-BMIPP for the diagnosis of coronary artery disease. *J Nucl Med*. 1997;38:175-180.
- Ishii Y, MacIntyre WJ, Pritchard WH, Eckstein RW. Measurement of total myocardial blood flow in dogs with 43K and the scintillation camera. *Circ Res*. 1973;33:113-122.
- Tamaki N, Yoheura Y, Kawamoto M, et al. Simple quantification of regional myocardial uptake of fluorine-18-deoxyglucose in the fasting condition. *J Nucl Med*. 1991;32:2152-2157.
- Scott WJ, Schwabe JL, Gupta NC, et al. Positron emission tomography of lung tumors and mediastinal lymph nodes using F-18-fluorodeoxyglucose. *Ann Thorac Surg*. 1994;58:698-703.
- Ikeda H, Mitani T, Ohnuma M, et al. A new platelet-specific antigen, Naka, involved in the refractoriness of HLA-matched platelet transfusion. *Vox Sanguinis*. 1989;57:213-217.
- Tomiyama Y, Take H, Ikeda H, et al. Identification of the platelet-specific alloantigen, Naka, on platelet membrane glycoprotein IV. *Blood*. 1990;75:684-687.
- DeGrella RF, Light RJ. Uptake and metabolism of fatty acids by dispersed adult rat heart myocytes. II. Inhibition by albumin and fatty acid homologues, and the effect of temperature and metabolic reagents. *J Biol Chem*. 1980;255:9739-9745.
- Rose H, Hennecke T, Kammermeier H. Sarcolemmal fatty acid transfer in isolated cardiomyocytes governed by albumin/membrane-lipid partition. *J Mol Cell Cardiol*. 1990;22:883-892.
- Stremmel W, Strohmeier G, Borchard F, Kochwa S, Berk PD. Isolation and partial characterization of a fatty acid binding protein in rat liver plasma membranes. *Proc Natl Acad Sci USA*. 1985;82:4-8.
- Stremmel W. Fatty acid uptake by isolated rat heart myocytes represents a carrier-mediated transport process. *J Clin Invest*. 1988;81:844-852.
- Harmon CM, Abumrad NA. Binding of sulfosuccinimidyl fatty acids to adipocyte membrane proteins: isolation and amino-terminal sequence of an 88-kDa protein implicated in transport of long-chain fatty acids. *J Membr Biol*. 1993;133:43-49.
- Morishita S, Kusuoka H, Yamamichi Y, Suzuki N, Kurami M, Nishimura T. Kinetics of radioiodinated species in subcellular fractions from rat hearts following administration of iodine-123-labelled 15-(p-iodophenyl)-3-(R,S)-methyl pentadecanoic acid (¹²³I-BMIPP). *Eur J Nucl Med*. 1996;23:383-389.
- Yamamichi Y, Kusuoka H, Morishita K, et al. Metabolism of iodine-123-BMIPP in perfused rat hearts. *J Nucl Med*. 1995;36:1043-1050.
- Tanaka T, Kawamura K. Isolation of myocardial membrane long-chain fatty acid-binding protein: homology with a rat membrane protein implicated in the binding or transport of long-chain fatty acids. *J Mol Cell Cardiol*. 1995;27:1613-1622.
- Knapp F, Goodman M, Ambrose K, et al. The development of iodine-123-methyl-branched fatty acids and their applications in nuclear cardiology. *Ann Nuclcardiol*. 1993;7:1-14.
- Hashimoto A, Nakata T, Tsuchihashi K, Tanaka S, Fujimori K, Iimura O. Postischemic functional recovery and BMIPP uptake after primary percutaneous transluminal coronary angioplasty in acute myocardial infarction. *Am J Cardiol*. 1996;77:25-30.
- Takeishi Y, Fujiwara S, Atsumi H, Takahashi K, Sukekawa H, Tomoike H. Iodine-123-BMIPP imaging in unstable angina: a guide for interventional strategy. *J Nucl Med*. 1997;38:1407-1411.
- Schelbert HR, Henze E, Phelps ME, Kuhl DE. Assessment of regional myocardial ischemia by positron-emission computed tomography. *Am Heart J*. 1982;103:588-597.
- Marshall RC, Tillisch JH, Phelps ME, et al. Identification and differentiation of resting myocardial ischemia and infarction in man with positron computed tomography, ¹⁸F-labeled fluorodeoxyglucose and ¹³N-ammonia. *Circulation*. 1983;67:766-778.